Physiological and transcriptional response of *Candida parapsilosis* to exogenous tyrosol

Running headline: Effect of tyrosol in *C. parapsilosis*

Ágnes Jakab[1], Zoltán Tóth[2], Fruzsina Nagy[2], Dániel Nemes[3], Ildikó Bácskay[3], Gábor Kardos[2], Tamás Emri[1], István Pócsi[1], László Majoros[2], Renátó Kovács[2,4*]

[1]Department of Molecular Biotechnology and Microbiology, Institute of Biotechnology, Faculty of Science and Technology, University of Debrecen, Debrecen, Hungary.

[2]Department of Medical Microbiology, Faculty of Medicine, University of Debrecen, Debrecen, Hungary

[3]University of Debrecen, Faculty of Pharmacy, Department of Pharmaceutical Technology, Debrecen, Hungary

[4]Faculty of Pharmacy, University of Debrecen, Debrecen, Hungary

*Corresponding author: Renátó Kovács; Department of Medical Microbiology, Faculty of Medicine, University of Debrecen, 4032 Debrecen, Nagyerdei krt. 98., Hungary, Phone: 00-36-52-255-425; e-mail: kovacs.renato@med.unideb.hu

Abstract

Tyrosol plays a key role in fungal morphogenesis and biofilm development. Also, it has a remarkable antifungal effect at supraphysiological concentrations. However, the background of the antifungal effect remains unknown, especially in the case of non-albicans *Candida* species such as *Candida parapsilosis*. We examined the effect of tyrosol on the growth, adhesion, redox homeostasis, virulence, as well as on fluconazole susceptibility. To gain further insights into the physiological consequences of tyrosol treatment we also determined the caused genome-wide gene expression changes using RNA-Seq. Fifteen mM tyrosol caused significant growth inhibition within two hours of the addition of tyrosol, while the adhesion of yeast cells was not affected. Tyrosol increased the production of reactive oxygen species remarkably as revealed by the dichlorofluorescein-test, and it was associated with elevated superoxide dismutase, glutathione peroxidase, and catalase activities. The interaction between fluconazole and tyrosol was antagonistic. Tyrosol exposure resulted in 261 and 181 differentially expressed genes with at least a 1.5-fold increase or decrease in expression, respectively, were selected for further study. Genes involved in ribosome biogenesis showed down-regulation, while genes related to oxidative stress response, and ethanol fermentation were up-regulated. In addition, tyrosol treatment up-regulated the expression of efflux pump genes including *MDR1* and *CDR1* and down-regulated the *FAD2* and *FAD3* virulence genes involved in desaturated fatty acid formation. Our data demonstrate that exogenous tyrosol significantly affects the physiology and gene expression of *C. parapsilosis*, which could contribute to the development of treatments targeting quorum-sensing in the future.

Importance

Candida-secreted quorum-sensing molecules (i.e., farnesol, tyrosol) are key regulators in fungal physiology, which induce phenotypic adaptations including morphological changes,

altered biofilm formation, and synchronized expression of virulence factors. Moreover, they have a remarkable antifungal activity at supraphysiological concentrations. Limited data are available concerning the tyrosol-induced molecular and physiological effects in non-albicans species such as *C. parapsilosis*. In addition, the background of the previously observed antifungal effect caused by tyrosol remains unknown. This study revealed that tyrosol exposure enhanced the oxidative stress response and expression of efflux pump genes, while it inhibited growth and ribosome biogenesis, as well as several virulence-related genes. Metabolism was changed towards glycolysis and ethanol fermentation. Furthermore, the initial adherence was not influenced significantly in the presence of tyrosol. Our results provide several potential explanations of the previously observed antifungal effect.

Keywords: *Candida parapsilosis*, tyrosol, quorum-sensing, RNA-Seq, oxidative stress

Introduction

The proliferation and virulence of *Candida* cells are under strict cell density-based control mediated by various quorum-sensing molecules including farnesol and tyrosol (1-2). While farnesol induces the hyphae-to-yeast transition in *Candida albicans*, tyrosol has an opposite effect. Tyrosol is a tyrosine derivative molecule, which is released into the growth medium continuously during the exponential growth phase and is capable of decreasing the duration of the lag phase before cells begin germination (3). Previous studies have reported that the accumulation of tyrosol in the culture medium is directly related to the increase in fungal cell density (3-4). Moreover, 20 μM tyrosol could stimulate the germ-tube and hypha formation in the early and intermediate stages of biofilm development (4). Based on the gene expression profile of *C. albicans*, tyrosol affects cell cycle regulation, DNA replication and chromosome segregation (3). Besides its role in fungal physiology, tyrosol also possess remarkable antifungal activity at supraphysiological concentrations (1 to 50 mM) both against planktonic and sessile *Candida* populations; therefore, its potential role in certain aspects of antifungal therapy has been postulated, e.g. in catheter-lock therapy (5-7).

In recent years, alternative treatments targeting quorum-sensing against *Candida* species has become an intensively researched area; however, tyrosol remains a mysterious molecule and the exact background of its antifungal mechanism is still poorly understood (1-2, 8-10). In the case of *C. albicans*, both the transcriptional and physiological responses exerted by tyrosol have been addressed earlier (3-4) aiding the understanding of the observed antifungal effect against *C. albicans*. However, the tyrosol-induced physiological and molecular events, especially in non-albicans species remained unknown so far. Hereby, we report the effect of tyrosol at supraphysiological concentration on cell growth, adhesion, oxidative stress - related enzyme production, virulence, fluconazole susceptibility, as well as on gene expression,

87 which may help understand the potential physiological and molecular background of its
88 antifungal effect in *C. parapsilosis*.
89

Materials and methods

Fungal strain, culture medium and epithelial cell line

The CLIB 214 *C. parapsilosis* (*sensu stricto*) reference strain was used in all experiments. The strain was maintained and cultured on Yeast Extract–Peptone–Dextrose (YPD) agar (1% yeast extract, 2% mycological peptone, 2% glucose, and 2% agar, pH 5.6). The Caco-2 epithelial cell line was cultured as described earlier by Nemes et al. 2018 (11). The Caco-2 cell line was obtained from the European Collection of Cell Cultures (ECACC, Salisbury, United Kingdom). Cells were grown in plastic cell culture flasks in Dulbecco's Modified Eagle's Medium (DMEM), supplemented with 3.7 g/L $NaHCO_3$, 10% (v/v) heat-inactivated fetal bovine serum, 1% (v/v) non-essential amino acids solution, 0.584 g/L L-glutamine, 4.5 g/L D-glucose, 100 IU/mL penicillin, and 100 mg/L streptomycin at 37 °C in the presence of 5% CO_2. The cells were routinely maintained by regular passaging and glutamine was supplemented by GlutaMax™. The cells used for adhesion and toxicity experiments were between passage numbers 20 and 40 (11).

Tyrosol (2-(4-hydroxyphenyl) ethanol, Sigma, Budapest, Hungary) was prepared as 0.1 M stock solution in YPD or sterile physiological saline for physiology experiments and susceptibility testing or *in vivo* experiments, respectively. The stock solution of fluconazole was prepared in sterile distilled water and preserved according to the manufacturer's instructions. The susceptibility testing of *C. parapsilosis* against tyrosol and fluconazole was performed using RPMI-1640 medium (with L-glutamine and without bicarbonate, pH 7.0 with 3-(N-morpholino) propanesulfonic acid (MOPS); Sigma, Budapest, Hungary).

Toxicity experiments

In preliminary experiments, 100 μM, 1 mM, 10 mM, and 15 mM tyrosol were evaluated in terms of toxicity on the Caco-2 cell line using MTT assay (Sigma, Budapest, Hungary) (11-

12) and the xCELLigence real time cell analysis (ACEA Biosciences, Inc., San Diego, USA) (13) where none of them caused relevant toxicity. As at 100 μM, 1 mM, and 10 mM tyrosol concentrations the caused physiological and transcriptional changes that were less marked in *C. parapsilosis*. We focused exclusively on the effect of 15 mM tyrosol in further experiments in order to reveal the potential mechanisms of the antifungal effect.

Growth conditions

The pre-cultures were grown in YPD medium at 30 ºC at 3.7 Hz shaking frequency for 18 hours then diluted to OD_{640} 0.2 value (corresponding to $2.9 \pm 0.5 \times 10^6$ colony forming unit (CFU)/mL) in 20 mL of YPD and incubated at 37 ºC with 2.3 Hz shaking frequency (14). Following four hours incubation time, we added 15 mM tyrosol to the YPD cultures then growth was examined at one-hour intervals by determination of cell density both by means of measuring of the absorbance (at 640 nm) and by counting the living cells (CFU) as described previously (15). Morphological alterations were monitored using phase-contrast microscopy (Euromex Holland) with the MicroQ-W PRO camera, which was used to evaluate the ratio of yeast and pseudohyphae based on 100 cells per sample. Statistical comparison of the growth-based data was performed by the paired Student's *t*-test using GraphPad Prism 6.05 software. The results between treated and control values were considered significant if the p-value was <0.05.

For reactive species production, antioxidant enzyme activities and RNA extraction, the yeast pre-cultures were diluted to 0.2 value (OD_{640}) in YPD broth then cultures were grown for four hours at 37 ºC. Then YPD medium was supplemented with a final concentration of 15 mM tyrosol and fungal cells were collected two hours following tyrosol exposure by centrifugation (5 min, RCF = 4000 g, 4 °C). The cells were washed three times with phosphate-buffered saline and stored at -70 °C until use (16).

Reactive species production and antioxidant enzyme activities

Reactive species were measured in the presence or absence of tyrosol by a technique that converts 2',7' –dichlorofluorescin diacetate to 2',7'–dichlorofluorescein (DCF) (Sigma, Budapest, Hungary). The produced DCF is directly proportional to the number of reactive species (16).

Glutathione reductase, glutathione peroxidase, catalase and superoxide dismutase activities were determined as described earlier by Jakab et al. (2015) (16). Reactive species and enzyme activities were measured in three independent experiments and presented as mean ± standard deviation. Statistical comparison of reactive species and enzyme production data were performed by the paired Student's *t*-test using GraphPad Prism 6.05 software. The results between treated and control values were considered significant if the p-value was <0.05.

Adhesion experiments

The Caco-2 epithelial cell line was inoculated with 1×10^5 CFU/mL *C. parapsilosis* in order to evaluate the adhesion of fungal cells as described previously (17-18). In the adhesion assay, Caco-2 and *C. parapsilosis* cells were co-incubated for one hour in DMEM medium at 37 °C in the presence of 5% CO_2 with and without 15 mM tyrosol. Afterwards, non-adherent fungal cells were removed by rinsing with phosphate-buffered saline, and the epithelial cells were fixed with 4% formaldehyde. Adherent *C. parapsilosis* cells were stained with calcofluor white (Sigma, Budapest, Hungary) and stained fungal cells were examined with a Zeiss AxioScope A1 fluorescence microscope with Zeiss AxioCam ICm1 camera (17-18). Adhesion (%) was calculated using the following formula: [(average cell count in the field × area of the well in μm^2) / (area of the field in μm^2 × inoculated fungal cells in each well)]×100. Adhesion was evaluated in three independent experiments and presented as the mean ± standard deviation. Statistical comparison of adhesion-related data was performed by

the paired Student's *t*-test using GraphPad Prism 6.05 software. The results between treated and control values were considered significant if the p-value was <0.05.

Evaluation of extracellular phospholipase and aspartic proteinase activity

Extracellular phospholipase production of tyrosol-treated and untreated *C. parapsilosis* cells was examined on egg yolk medium [5.85% (w/v) NaCl, 0.05% (w/v) $CaCl_2$ and 10% (v/v) sterile egg yolk (Sigma, Budapest, Hungary) in YPD medium]. Aspartic proteinase activity was evaluated on a solid medium supplemented with bovine serum albumin (Sigma, Budapest, Hungary).

According to Kantarcioglu and Yücel (2002), 5 μL of 1×10^7 cells/mL suspensions were inoculated onto the surface of the agar plates (19). Colony diameters and the colony + precipitation zones were measured after seven days of incubation at 37 °C (20).

Biofilm formation

C. parapsilosis one-day-old biofilms were prepared as described previously (6, 21). Briefly, isolates were suspended in RPMI-1640 broth in concentration of 1×10^6 cells/mL and aliquots of 100 μL were inoculated onto flat-bottom 96-well sterile microtitre plates (TPP, Trasadingen, Switzerland) in the presence or absence of 15 mM tyrosol and then incubated statically at 37°C for 24 hours (6, 21). One-day-old biofilm formation ability was determined by quantitative CFU determination of adhered cells and metabolic activity measurement using the XTT-assay (2,3-Bis-(2-methoxy-4-nitro-5-sulfophenyl)-2H-tetrazolium-5-carboxanilide salt) (6, 21). Statistical comparison of CFU data and metabolic activity change between tyrosol-treated and untreated cells was performed by the Mann-Whitney test using the GraphPad Prism 6.05 software. The results between treated and control values were considered significant if the p-value was <0.05.

Susceptibility testing to fluconazole and tyrosol against planktonic cells and biofilms

Planktonic minimum inhibitory concentration (MIC) determination was performed in line with the guideline of the M27-A3 document published by the Clinical Laboratory Standards Institute (22). MICs of fluconazole and tyrosol were determined in RPMI-1640. The tested drug concentrations ranged from 0.03 to 2 mg/L for fluconazole, while tyrosol concentrations ranged from 0.5 to 60 mM. MICs were determined as the lowest drug concentration that produces at least 50% growth reduction compared to growth control (22). MICs represent three independent experiments per isolate and are expressed as the median.

The examined concentrations for sessile MIC determination (sMIC) ranged from 0.125 to 8 mg/L and from 0.5 to 60 mM for fluconazole and tyrosol, respectively. The preformed biofilms were washed three times with sterile physiological saline. Different drug concentrations in RPMI-1640 were added to biofilms and then the plates were incubated for 24 hours at 37 °C Afterwards, sMIC determination was performed using the XTT-assay as described previously (6, 21). The percentage change in metabolic activity was calculated on the basis of absorbance (A) at 492 nm as $100\% \times (A_{well}\text{-}A_{background})/(A_{drug\text{-}free\ well}\text{-}A_{background})$. sMICs of the biofilms were defined as the lowest drug concentration resulting in at least 50% metabolic activity reduction compared to growth control cells (6, 21). sMICs represent three independent experiments per isolate and are expressed as the median value.

Evaluation of interactions of fluconazole and tyrosol by fractional concentration index (FICI)

Interaction between fluconazole and tyrosol was evaluated by the two-dimensional broth microdilution chequerboard assay against planktonic and sessile cells. Afterwards, the nature of the interaction was analysed using FICI determination. The tested concentration ranges

were the same as described above for the MIC determination. FICIs were calculated using the following formula: $\Sigma FIC = FIC_A + FIC_B = MIC_A^{comb}/MIC_A^{alone} + MIC_B^{comb}/ MIC_B^{alone}$, where MIC_A^{alone} and MIC_B^{alone} stand for MICs of drugs A and B when used alone, and MIC_A^{comb} and MIC_B^{comb} represent the MIC values of drugs A and B at isoeffective combinations, respectively (21, 23). FICIs were determined as the lowest ΣFIC. FICI values of ≤ 0.5 were defined as synergistic, between >0.5 and 4 as indifferent, and >4 as antagonistic. FICIs were determined in three independent experiments and median values were presented (21, 23).

***In vivo* experiments**

Groups of twelve BALB/C female mice (19-22g) were maintained in accordance with the Guidelines for the Care and Use of Laboratory Animals; experiments were approved by the Animal Care Committee of the University of Debrecen (permission no.: 12/2014 DEMÁB). Mice were immunosuppressed with four doses of intraperitoneal cyclophosphamide, i.e., four days prior to infection (150 mg/kg), one day prior to infection (100 mg/kg), two days post-infection (100 mg/kg) and five days post-infection (100 mg/kg) (15). Mice were inoculated intravenously through the lateral tail vein with an infectious dose of 7×10^6 CFU/mouse. The inoculum density was confirmed by plating serial dilutions onto Sabouraud dextrose agar plates. A five-day intraperitoneal treatment with daily 15 mM tyrosol was started 24 hours post-inoculation. On day six after infection, all mice were sacrificed, kidneys were removed, weighed, and homogenised aseptically. Homogenates were diluted 10-fold; aliquots of 0.1 mL of the undiluted and diluted homogenates were plated onto Sabouraud dextrose agar plates and incubated at 37 ^oC for 48 hours. The lower limit of detection was 50 CFU/g of tissue. Statistical analysis of the kidneys tissue burden was performed using an unpaired *t*-test (15). Kidney burden was analyzed using Kruskal-Wallis test with Dunn's post-test (GraphPad Prism 6.05.). Significance was defined as $p < 0.05$.

RNA sequencing

Total RNA was isolated from untreated control fungal cells and 15 mM tyrosol-treated cultures in three replicates. Freeze-dried cells were processed using TRISOL (Invitrogen, Austria) reagent according to Chomczynski (1993) (24).

To obtain global transcriptome data, high-throughput mRNA sequencing was performed on an Illumina NextSeq sequencing platform. Total RNA sample quality was checked on an Agilent BioAnalyzer using the Eukaryotic Total RNA Nano Kit (Agilent Technologies, Inc., Santa Clara, CA, USA) according to the manufacturer's protocol. Samples with RNA integrity number (RIN) value >7 were accepted for the library preparation process. RNA-Seq libraries were prepared from the total RNA using the TruSeq RNA Sample preparation kit (Illumina, San Diego, CA, USA) according to the manufacturer's protocol. Sequencing libraries were normalised to the same molar concentration and pooled together. The library pool was sequenced on NextSeq500 instrument (Illumina, San Diego, CA, USA) generating single read 75bp-long sequencing reads. Fastq files were generated automatically after the sequencing run by Illumina BaseSpace. The library preparations and the sequencing run were performed by the Genomic Medicine and Bioinformatics Core Facility of the Department of Biochemistry and Molecular Biology, Faculty of Medicine, University of Debrecen, Hungary. Quality control of the sequencing data was performed using the FastQC package (http://www.bioinformatics.babraham.ac.uk/projects/fastqc) then the STAR RNA-Seq aligner was used to map the sequenced reads to the reference genome (*C_parapsilosis*_CDC317_version_s01m03r27_features_with_chromosome_sequences.gff.gz ;http://www.candidagenome.org/download/gff/C_parapsilosis_CDC317/archive/). The DESeq algorithm (StrandNGS software) was used to obtain normalised gene expression (FPKM, fragments per kilobase per million mapped fragments) values. Gene expression

differences between treated and control groups were compared by moderated *t*-test; Benjamini-Hochberg False Discovery Rate was used for multiple testing correction and a corrected $p < 0.05$ was considered significant (differentially expressed genes). Up- and down-regulated genes were defined as differentially expressed genes with more than 1.5-fold change (FC) values. The FC ratios were calculated from the FPKM values.

Reverse transcriptase-quantitative polymerase chain reaction (RT-qPCR) assays

To confirm the RNA-Seq results, ten up-regulated and six down-regulated genes, as well as nine genes without significant change in their expression were selected for the RT-qPCR analysis.

The RT-qPCRs with Xceed qPCR SG 1-step 2x Mix Lo-ROX kit (Institute of Applied Biotechnologies, Czech Republic) were performed according to the protocol of the manufacturer using 500 ng of DNase- (Sigma, Budapest, Hungary) treated total RNA per reaction.

Primer pairs (Table S1) were designed using OligoExplorer (version 1.1.) and Oligo Analyser (version 1.0.2) software and were purchased from Integrated DNA Technologies. Three parallel measurements were performed with each sample in a LightCycler® 480 II real-time PCR instrument (Roche, Switzerland) (25). Relative transcription levels were quantified with ΔΔCP values. $\Delta\Delta CP = \Delta CP_{control} - \Delta CP_{treated,}$ where $\Delta CP_{treated} = CP_{tested\ gene} - CP_{reference\ gene}$ measured from treated cultures and $\Delta CP_{control} = CP_{tested\ gene} - CP_{reference\ gene}$ measured from control cultures. CP values represented the qRT-PCR cycle numbers of crossing points. Three reference genes (*ACT1, TUB2, TUB4*) were tested. All of them showed stable transcription in our experiments. Only data calculated with the *ACT1* (CPAR2_201570**)** transcription values are presented. ΔΔCP values are expressed as mean ± SD calculated from three independent

289 measurements and ΔΔCP values significantly ($p < 0.05$) higher or lower than zero were
290 determined using the Student's *t*-test (25).
291
292 **Gene set enrichment analysis.**
293 Significant shared GO (gene ontology) terms were determined with the Candida Genome
294 Database Gene Ontology Term Finder (http://www.candidagenome.org/cgi-
295 bin/GO/goTermFinder). Only hits with an adjusted p-value <0.05 were taken into
296 consideration during the evaluation process.
297
298

Results

Effect of tyrosol on growth, morphology, extracellular phospholipase, and proteinase production, biofilm formation as well as adhesion to Caco-2 cells.

Growth of *C. parapsilosis* was examined following 15 mM tyrosol exposure in YPD. Adding tyrosol to preincubated cells resulted in a significant inhibition starting at six hours post-inoculation, which was confirmed both by absorbance measurements and CFU determination. Growth was significantly inhibited within two hours of the addition of tyrosol both in terms of CFU change ($8.25 \pm 0.8 \times 10^7$ and $4.5 \pm 0.4 \times 10^7$ CFU/mL for untreated control and tyrosol-exposed cells, respectively) ($p = 0.002$), and of observed absorbance values (OD_{640}) ($p = 0.002$) (Fig. 1). The ratio of yeast and pseudohyphae was comparable between control (69.3 ± 2.1% and 28.7 ± 3.5% for yeast and pseudohyphae, respectively) and treated cells (66.0 ± 1.7% and 37.7 ± 1.5% for yeast and pseudohyphae, respectively) at two hours stress exposure time ($p > 0.05$). Tyrosol treatment did not influence significantly the extracellular proteinase activity (Pz values were 0.82 ± 0.04 and 0.80 ± 0.05 for untreated control and tyrosol-exposed cells, respectively $p > 0.05$). There was no remarkable phospholipase activity for untreated control and tyrosol-exposed cells (Pz value was 1.0), respectively. Biofilm forming ability was comparable with and without 15 mM tyrosol ($4.9 \pm 1.1 \times 10^5$ and $6.4 \pm 1.9 \times 10^5$ living fungal cells at 24 hours for untreated control and tyrosol-exposed cells, respectively) ($p > 0.05$); however, metabolic activity was significantly increased in the tyrosol treatment group ($p = 0.001$). Adhesion of *C. parapsilosis* to Caco-2 cells in the presence of tyrosol (4.2 ± 1.1% adherent cells) did not differ significantly from that observed with untreated control cells (3.1 ± 1.1% adherent cells) ($p > 0.05$).

Tyrosol-induced oxidative stress and stress response in *C. parapsilosis*

Tyrosol caused significantly higher reactive species production compared to untreated control cells ($p < 0.001$) as presented in Table 1. This tyrosol-related higher reactive species level was associated with elevated superoxide dismutase ($p = 0.021$), glutathione peroxidase ($p = 0.012$) and catalase activities ($p = 0.013$) in tyrosol-exposed cells (Table 1). In contrast, the measured glutathione reductase values were statistically comparable ($p > 0.05$) in tyrosol-treated and untreated *Candida* cells (Table 1).

Susceptibility to fluconazole and tyrosol for planktonic and sessile *C. parapsilosis*

The median planktonic MICs of fluconazole and tyrosol were 0.5 mg/L and 30 mM, respectively. FICI determination showed clear antagonistic interaction; the median FICI value of three independent experiments was 4.125. In case of the biofilms, the median MIC values were 4 mg/L and 30 mM for fluconazole and tyrosol, respectively, while the interaction was also antagonistic (FICI 4.5), similar that of the planktonic cells.

***In vivo* experiments**

The daily treatment of 15 mM tyrosol decreased the fungal tissue burden in the kidneys at least by half a log degree, which corresponded to a significantly lower tissue burden ($p = 0.004$) than seen in the untreated control (Fig. 2).

Transcriptional profiling and RNA-Seq data validation

Comparison of tyrosol-treated *C. parapsilosis* cells gene expression profile with that of untreated cells revealed 1,462 differentially expressed genes (Fig. S1). The qRT-PCR data of the selected 25 genes showed a strong correlation with the obtained RNA-Seq data (Fig. 3 and Table S2).

Tyrosol responsive genes were defined as differentially expressed genes with $\log_2$(FC)>0.585 (up-regulated genes) or $\log_2$(FC)< –0.585 (down-regulated genes), where FC stands for fold change FPKM value (tyrosol treated *vs*. untreated cultures). Results of the gene set enrichment analysis of the 261 up-regulated and 181 down-regulated genes are presented in Table 2, S3, and S4 and summarised as below.

Evaluation of tyrosol responsive genes

Virulence-related genes

Selected genes involved in genetic control of *C. parapsilosis* virulence were determined according to Tóth et al. (2019) (26). Virulence-related genes were significantly enriched within the tyrosol responsive up-regulated gene group according to the Fisher's exact test (Table S4). Most of these 16 putative genes are involved in the biofilm production (*e.g., CZF1*, *RBT1*, *IFD6*, *TEC1*, *HGC1*, *NRG1*) (Fig. 4, Table 2, Tables S3 and S4). Out of the three down-regulated virulence-related genes, *FAD2* and *FAD3* (involved in saturated fatty acid formation) and *MKC1* (a putative regulator of biofilm formation) are notable (Fig. 4, Table 2, Tables S3 and S4). It is noteworthy that tyrosol may also enhance its production through increasing the gene expression level of *ADH5*, which is involved in the tyrosine–tyrosol conversion in *C. albicans* and in *Saccharomyces cerevisiae* (27).

Cell wall-related genes

Regarding cell wall assembly, the expression level of the putative genes *PDC11*, *TDH3*, *ADH1* were upregulated by tyrosol treatment (Fig. 4, Table 2, Tables S3 and S4).

Antifungal drug transport-related genes

Significant up-regulation of putative genes encoding antifungal drug transport proteins were observed (*e.g., MDR1, CDR1, FCR1*) (Fig. 4, Table 2, Tables S3 and S4).

Metabolic pathway-related genes

Selected genes involved in glucose catabolism were determined with the Candida Genome Database (http://www.candidagenome.org). Tyrosol exposure resulted in increased expression of several genes related to the "carbohydrate metabolic process" GO term including glycolysis (*PGI1*, *PFK1*, *PFK2*, *TDH3*, *PGK1*, *GPM2*, *ENO1*, *CDC19*) and fermentation (*PDC11*, *PDC12*, *ADH1*, *ADH5*, *ADH7*) genes but not the tricarboxylic acid cycle genes (Fig. 4, Table 2, Tables S3 and S4). In contrast, tyrosol treatment led to a reduced expression of several genes (altogether 42 gene) involved in the transmembrane transport, including 10 putative carbohydrate transport genes and 12 putative amino acid transport genes (Fig. 4, Table 2, Tables S3 and S4). Down-regulation of ribosome biogenesis genes (altogether 36 genes) was also notable (Fig. 4, Table 2, Tables S3 and S4).

Oxidative stress-related genes

Genes belonging to the "response to oxidative stress" GO term were enriched in the tyrosol-responsive up-regulated gene group (Fig. 4, Table 2, Tables S3 and S4). Altogether 18 genes were up-regulated after tyrosol treatment including *CAT1*, *SOD4*, *CPAR2_803850*, *GPX1*, *GST2*, *AHP1*, *CAP1*, *PST1*, *CIP1*, *TAC1*, *MSN4*, (Fig. 4, Table 2, Tables S3 and S4).

Discussion

Alternative treatments targeting fungal quorum-sensing has become an intensely researched area in the recent years (1-2, 5-8, 10). However, the majority of studies focused on farnesol-related antifungal effects especially in the case of *C. albicans* (1, 10). Therefore, there are limited data about tyrosol-induced changes particularly among non-albicans species such as *C. parapsilosis*, which is the second most frequently isolated *Candida* species from blood in Asia, Latin-America, and several Mediterranean European countries (28).

Previous studies reported that tyrosol has a potential antifungal effect similar to farnesol (5-7, 29-31); moreover, it enhances the activity of caspofungin and micafungin against *C. parapsilosis* (6). Nevertheless, the exact physiological and transcriptional background of antifungal activity exerted by tyrosol remains to be elucidated. In the present study, tyrosol exposure was associated with physiological alterations as well as genome-wide transcriptional changes in *C. parapsilosis*.

Concerning our growth-based experiments, a significant inhibitory effect was induced by the tyrosol concentration used, which is in line with previous investigations concerned with *C. albicans*, *C. tropicalis*, and *C. krusei* (5, 7, 29). The observed significant down-regulation of ribosome biogenesis genes is concordant with this marked growth inhibition. Another explanation for the antifungal effect of tyrosol is the induction of oxidative stress suggested by the increased level of reactive species in the presence of tyrosol. These reactive species can alter the ratio of saturated and unsaturated fatty acids in the cell membrane; furthermore, hydrogen peroxide and hydroxyl radicals cause irreversible damage to proteins, lipids and nucleic acids resulting in impaired viability (30). A well-known response of fungal species to reactive oxygen species is the rapid induction of oxidative stress detoxification at the mRNA level (30). In this study, several putative oxidative stress-responsive genes, *CAT1*, CPAR2_803850 (both coding for catalase activity), *GPX1* (encoding for glutathione

peroxidase) and *SOD4* (encoding for superoxide dismutase), were up-regulated following exposure to tyrosol, which was associated with increased catalase, glutathione peroxidase and superoxide dismutase activities. Furthermore, *CAP1*, the major transcription factor in oxidative stress elimination, was also overexpressed following tyrosol exposure (30).

The elevated levels of the reactive species may be explained by the disruption of polyunsaturated fatty acid (PUFA) metabolism. The synthesis of PUFAs is significantly down-regulated in tyrosol-treated cells, as tyrosol decreased the expression of genes *FAD2* and *FAD3* encoding delta12-fatty acid desaturase and omega-3 fatty acid desaturase enzymes, respectively. These are orthologs of genes participating in PUFA synthesis in *C. albicans* (31-32). PUFAs (stearidonic acid, eicosapentaenoic acid and docosapentaenoic acid) are major components of the cell membrane in *C. parapsilosis*, accounting for approximately 30% of the fatty acid content, and have a remarkable antioxidant effect (32). Tyrosol-induced inhibition of the expression of *FAD2* and *FAD3* found in this study, therefore, decreases the antioxidant level in cell membranes, which may contribute to the antifungal effect of tyrosol against *C. albicans* or *C. parapsilosis* (31-33). Although tyrosol was reported to exert an antioxidant effect, this was only measured at micromolar concentration (34), while the concentration used in this study was 15 mM.

Tyrosol is a well-known regulator molecule in the biofilm formation of *C. albicans* (3-4); however, its exact role in the development of *C. parapsilosis* biofilms remained unknown. In this study, the ortholog of the *C. albicans CZF1* gene, which is one of the key transcription factor of biofilm development in the *C. parapsilosis*, was up-regulated following the tyrosol exposure (35). *CZF1* promotes the yeast-to-pseudohyphae transition (35); *CZF1* mutants formed reduced colony wrinkling and the biofilms produced contained mainly yeast cells (35). Nonetheless, we did not observe higher rate of adherence and biofilm-forming ability in the presence of tyrosol. Monteiro et al. (2015) observed that tyrosol did not induce increased

adhesion in *C. albicans* and *C. glabrata*, which is in line with the gene expression pattern observed and the biofilm formation experiments in our study with *C. parapsilosis* (36). Tyrosol had no effect on putative morphology-related genes (*CPH2*, *EFG1*, *UME6*, *OCH1*, *SPT3*, *CWH41*), which is in line with our microscopic observations.

Regarding antifungal susceptibility, a clear antagonistic interaction was observed between fluconazole and tyrosol both against planktonic cells and biofilms. Tyrosol increased the expression of *MDR1* and *CDR1* orthologs, as well as the *FCR1*, C1_00830W, and *CPAR2_405280* drug transporter genes in *C. parapsilosis*, which may explain the observed antagonistic interactions. In contrast, in previous studies, farnesol exposure decreased the expression level of *MDR1* and *CDR1* as well as *ERG* genes, which was associated with the observed reversion of azole resistance in *C. albicans* (37-38). In *C. parapsilosis*, neither *MDR1* nor *CDR1* genes were influenced by farnesol (39). Furthermore, ergosterol biosynthesis genes were not affected by tyrosol; therefore, the observed antagonistic interaction was probably not linked to the ergosterol pathway but was rather due to the overexpression of the abovementioned efflux pumps.

Based on our *in vivo* experiments, the daily intraperitoneal treatment with 15 mM tyrosol for five days significantly reduced the fungal kidney burden in systemic infection with CLIB 214, which was in parallel with the results of the gene expression pattern. The transcriptional profiling showed that genes involved in adhesion (*ALS6*) had reduced expression in response to tyrosol. In addition, genes encoding secreted aspartyl proteinases (*SAPP1* and *SAPP3)* (40) were not up-regulated significantly, which may explain the above-mentioned decreased *in vivo* virulence. Furthermore, down-regulation of the expression of *FAD2* and *FAD3* coding for proteins involved in PUFA synthesis may also contribute to lower virulence by decreasing the tolerance for oxidative stress.

To the best of our knowledge, this is the first study analysing changes in gene expression in *C. parapsilosis* following tyrosol exposure using RNA-Seq (26), providing important insights into the mechanism of antifungal action of tyrosol and the response of *C. parapsilosis*, which may aid in the better understanding of tyrosol-related antifungal activity in non-albicans species. In summary, tyrosol exposure enhanced the oxidative stress response and up-regulated efflux pumps, while inhibiting growth and ribosome biogenesis as well as virulence. Metabolism was modulated towards glycolysis and ethanol fermentation. Initial adherence was not influenced by the presence of tyrosol. Our findings suggest that tyrosol may be a potential locally active and/or adjuvant agent in the development of alternative treatments targeting quorum-sensing against *C. parapsilosis* in the future.

Acknowledgements

Renátó Kovács was supported by the EFOP-3.6.3-VEKOP-16-2017-00009 program. Ágnes Jakab was supported by the NTP-NFTÖ-18 scholarship program. Zoltán Tóth and Fruzsina Nagy were supported by the ÚNKP-18-3 New National Excellence Program of the Ministry of Human Capacities. The research was financed by the European Union and the European Social Fund through the project EFOP-3.6.1–16–2016-00022 and by the Higher Education Institutional Excellence Program of the Ministry of Human Capacities in Hungary, within the framework of the Biotechnology thematic program of the University of Debrecen.

Conflict of interest

L. Majoros received conference travel grants from MSD, Astellas and Pfizer. All other authors declare no conflicts of interest.

Funding

Not applicable

Ethical approval

Not required

Availability of data and materials

The data discussed have been deposited in NCBI's Gene Expression Omnibus (41) (GEO; http://www.ncbi.nlm.nih.gov/geo/) and are accessible through GEO Series accession number GSE129372 (https://www.ncbi.nlm.nih.gov/geo/query/acc.cgi?acc=GSE129372).

References

1. Polke M, Leonhardt I, Kurzai O, Jacobsen ID. 2018. Farnesol signalling in *Candida albicans* - more than just communication. Crit Rev Microbiol 44: 230-243.

2. Wongsuk T, Pumeesat P, Luplertlop N. 2016. Fungal quorum sensing molecules: Role in fungal morphogenesis and pathogenicity. J Basic Microbiol 56: 440-447.

3. Chen H, Fujita M, Feng Q, Clardy J, Fink GR. 2004. Tyrosol is a quorum-sensing molecule in *Candida albicans*. Proc Natl Acad Sci U S A 101:5048-5052

4. Alem MA, Oteef MD, Flowers TH, Douglas LJ. 2006. Production of tyrosol by *Candida albicans* biofilms and its role in quorum sensing and biofilm development. Eukaryot Cell 5: 1770-1779

5. Monteiro DR, Arias LS, Fernandes RA, Deszo da Silva LF, de Castilho MOVF, da Rosa TO, Vieira APM, Straioto FG, Barbosa DB, Delbem ACB. 2017. Antifungal activity of tyrosol and farnesol used in combination against *Candida* species in the planktonic state or forming biofilms. J Appl Microbiol 123:392-400

6. Kovács R, Tóth Z, Nagy F, Daróczi L, Bozó A, Majoros L. 2017. Activity of exogenous tyrosol in combination with caspofungin and micafungin against *Candida parapsilosis* sessile cells. J Appl Microbiol 122: 1529-1536

7. Shanmughapriya S, Sornakumari H, Lency A, Kavitha S, Natarajaseenivasan K. 2014. Synergistic effect of amphotericin B and tyrosol on biofilm formed by *Candida krusei* and *Candida tropicalis* from intrauterine device users. Med Mycol 52: 853-861

8. Padder SA, Prasad R, Shah AH. 2018. Quorum sensing: A less known mode of communication among fungi. Microbiol Res 210:51-58

9. Grainha TRR, Jorge PADS, Pérez-Pérez M, Pérez Rodríguez G, Pereira MOBO, Lourenço AMG. 2018. Exploring anti-quorum sensing and anti-virulence based strategies to fight *Candida albicans* infections: an in silico approach. FEMS Yeast Res 18

10. Polke M, Jacobsen ID. 2017. Quorum sensing by farnesol revisited. Curr Genet 63:791-797.

11. Nemes D, Kovács R, Nagy F, Mező M, Poczok N, Ujhelyi Z, Pető Á, Fehér P, Fenyvesi F, Váradi J, Vecsernyés M, Bácskay I. 2018. Interaction between Different Pharmaceutical Excipients in Liquid Dosage Forms-Assessment of Cytotoxicity and Antimicrobial Activity. Molecules 23 pii: E1827.

12. Berridge MV, Herst PM, Tan AS. 2005. Tetrazolium dyes as tools in cell biology: new insights into their cellular reduction. Biotechnol Annu Rev 11:127-152

13. Atienza JM, Zhu J, Wang X, Xu X, Abassi Y. 2005. Dynamic monitoring of cell adhesion and spreading on microelectronic sensor arrays. J Biomol Screen 10:795-805

14. Tóth R, Alonso MF, Bain JM, Vágvölgyi C, Erwig LP, Gácser A. 2015. Different *Candida parapsilosis* clinical isolates and lipase deficient strain trigger an altered cellular immune response. Front Microbiol 6:1102.

15. Kovács R, Gesztelyi R, Berényi R, Domán M, Kardos G, Juhász B, Majoros L. 2014. Killing rates exerted by caspofungin in 50 % serum and its correlation with in vivo efficacy in a neutropenic murine model against *Candida krusei* and *Candida inconspicua*. J Med Microbiol 63:186-194.

16. Jakab Á, Emri T, Sipos L, Kiss Á, Kovács R, Dombrádi V, Kemény-Beke Á, Balla J, Majoros L, Pócsi I. 2015. Betamethasone augments the antifungal effect of menadione--towards a novel anti-*Candida albicans* combination therapy. J Basic Microbiol 55:973-981

17. Dalle F, Wächtler B, L'Ollivier C, Holland G, Bannert N, Wilson D, Labruère C, Bonnin A, Hube B. 2010. Cellular interactions of *Candida albicans* with human oral epithelial cells and enterocytes. Cell Microbiol 12:248-271

549 **18.** Jakab Á, Mogavero S, Förster TM, Pekmezovic M, Jablonowski N, Dombrádi V, Pócsi I,
550 Hube B. 2016. Effects of the glucocorticoid betamethasone on the interaction of *Candida*
551 *albicans* with human epithelial cells. Microbiology 162:2116-2125
552 **19.** Kantarcioglu AS, Yücel A. 2002. Phospholipase and protease activities in clinical
553 *Candida* isolates with reference to the sources of strains. Mycoses 45:160-165.
554 **20.** Price MF, Wilkinson ID, Gentry LO. 1982. Plate method for detection of phospholipase
555 activity in *Candida albicans*. Sabouraudia 20:7–14.
556 **21.** Kovács R, Bozó A, Gesztelyi R, Domán M, Kardos G, Nagy F, Tóth Z, Majoros L. 2016.
557 Effect of caspofungin and micafungin in combination with farnesol against *Candida*
558 *parapsilosis* biofilms. Int J Antimicrob Agents 47:304-310.
559 **22.** Clinical and Laboratory Standards Institute. Reference method for broth dilution
560 antifungal susceptibility testing of yeasts. Approved standard, 3rd ed. M27-A3. CLSI, Wayne,
561 PA, USA 2008.
562 **23.** Meletiadis J, Verweij PE, TeDorsthorst DT, Meis JF, Mouton JW. 2005. Assessing *in*
563 *vitro* combinations of antifungal drugs against yeasts and filamentous fungi: comparison of
564 different drug interaction models. Med Mycol 43: 133-152.
565 **24.** Chomczynski P. 1993. A reagent for the single-step simultaneous isolation of RNA, DNA
566 and proteins from cell and tissue samples. Biotechniques 15:532-534
567 **25.** Kurucz V, Kiss B, Szigeti ZM, Nagy G, Orosz E, Hargitai Z, Harangi S, Wiebenga A, de
568 Vries RP, Pócsi I, Emri T. 2018. Physiological background of the remarkably high Cd2+
569 tolerance of the *Aspergillus fumigatus* Af293 strain. J Basic Microbiol 58:957-967
570 **26.** Tóth R, Nosek J, Mora-Montes HM, Gabaldon T, Bliss JM, Nosanchuk JD, Turner SA,
571 Butler G, Vágvölgyi C, Gácser A. 2019. *Candida parapsilosis*: from Genes to the Bedside.
572 Clin Microbiol Rev 32. pii: e00111-18.

573 **27.** Ghosh S, Kebaara BW, Atkin AL, Nickerson KW. 2008. Regulation of aromatic alcohol
574 production in *Candida albicans*. Appl Environ Microbiol. 74:7211-7218.
575 **28.** Cattana ME, Dudiuk C, Fernández M, Rojas F, Alegre L, Córdoba S, Garcia-Effron G,
576 Giusiano G. 2017. Identification of *Candida parapsilosis* Sensu Lato in Pediatric Patients and
577 Antifungal Susceptibility Testing. Antimicrob Agents Chemother 61: pii: e02754-16.
578 **29.** Cordeiro Rde A, Teixeira CE, Brilhante RS, Castelo-Branco DS, Alencar LP, de Oliveira
579 JS, Monteiro AJ, Bandeira TJ, Sidrim JJ, Moreira JL, Rocha MF. 2015. Exogenous tyrosol
580 inhibits planktonic cells and biofilms of *Candida* species and enhances their susceptibility to
581 antifungals. FEMS Yeast Res 15:fov012.
582 **30.** Dantas Ada S, Day A, Ikeh M, Kos I, Achan B, Quinn J. 2015. Oxidative stress responses
583 in the human fungal pathogen, *Candida albicans*. Biomolecules 5:142-165.
584 **31.** Thibane VS, Ells R, Hugo A, Albertyn J, van Rensburg WJ, Van Wyk PW, Kock JL, Pohl
585 CH. 2012. Polyunsaturated fatty acids cause apoptosis in *C. albicans* and *C. dubliniensis*
586 biofilms. Biochim Biophys Acta 1820:1463-1468.
587 **32.** Bucek A, Matouskova P, Sychrova H, Pichova I, Hruskova-Heidingsfeldova O. 2014.
588 Delta12-fatty acid desaturase from *Candida parapsilosis* is a multifunctional desaturase
589 producing a range of polyunsaturated and hydroxylated fatty acids. PLoS One 9:e93322.
590 **33.** Andrisic L, Collinson EJ, Tehlivets O, Perak E, Zarkovic T, Dawes IW, Zarkovic N,
591 Cipak Gasparovic A. 2015. Transcriptional and antioxidative responses to endogenous
592 polyunsaturated fatty acid accumulation in yeast. Mol Cell Biochem. 399:27-37.
593 **34.** Cremer J, Vatou V, Braveny I. 1999. 2,4-(hydroxyphenyl)-ethanol, an antioxidative agent
594 produced by *Candida* spp., impairs neutrophilic yeast killing *in vitro*. FEMS Microbiol Lett
595 170:319-325.

596 **35.** Holland LM, Schroder MS, Turner SA, Taff H, Andes D, Grozer Z, Gacser A, Ames L,
597 Haynes K, Higgins DG, Butler G. 2014. Comparative phenotypic analysis of the major fungal
598 pathogens *Candida parapsilosis* and *Candida albicans*. PLoS Pathog 10:e1004365.
599 **36.** Monteiro DR, Feresin LP, Arias LS, Barão VA, Barbosa DB, Delbem AC. 2015. Effect of
600 tyrosol on adhesion of *Candida albicans* and *Candida glabrata* to acrylic surfaces. Med
601 Mycol 53:656-665.
602 **37.** Jabra-Rizk MA, Shirtliff M, James C, Meiller T. 2006. Effect of farnesol on *Candida*
603 *dubliniensis* biofilm formation and fluconazole resistance. FEMS Yeast Res 6:1063-1073.
604 **38** Sharma M, Prasad R. 2011. The Quorum-Sensing Molecule Farnesol Is a Modulator of
605 Drug Efflux Mediated by ABC Multidrug Transporters and Synergizes with Drugs in
606 *Candida* albicans. Antimicrob Agents Chemother 55: 4834–4843.
607 **39.** Rossignol T, Logue ME, Reynolds K, Grenon M, Lowndes NF, Butler G. 2007.
608 Transcriptional response of *Candida parapsilosis* following exposure to farnesol. Antimicrob
609 Agents Chemother 51:2304-2312.
610 **40.** Horvath P, Nosanchuk JD, Hamari Z, Vagvolgyi C, Gacser A. 2012. The identification of
611 gene duplication and the role of secreted aspartyl proteinase 1 in *Candida parapsilosis*
612 virulence. J Infect Dis 205:923–933.
613 **41.** Edgar R, Domrachev M, Lash AE. 2002. Gene Expression Omnibus: NCBI gene
614 expression and hybridization array data repository. Nucleic Acids Res 30:207-210.
615

Table 1 Tyrosol-induced oxidative stress response in *Candida parapsilosis*

Oxidative stress related parameter	Untreated cultures	Tyrosol-treated cultures
Catalase [kat (kg protein)$^{-1}$]	1.4 ± 0.24	2.2 ± 0.4 *
GR [mkat (kg protein)$^{-1}$]	8.9 ± 0.4	9.6 ± 0.5
GPx [mkat (kg protein)$^{-1}$]	1.8 ± 0.3	2.5 ± 0.4 *
SOD [munit (mg protein)$^{-1}$]	72.5 ± 4.5	129.4 ± 10.9 *
DCF [nmol DCF (OD_{640})$^{-1}$]	11.7 ± 2	19.3 ± 2 ***

Mean ± standard deviation values calculated from three independent experiments are presented.

*, *** Significant differences at $p<0.05$ and 0.001, respectively, as calculated by the paired Student's *t*-test compared to untreated control and tyrosol-treated cultures.

Table 2 Summary of selected significant shared Gene Ontology (GO) terms.

Comparison	Up-regulated genes[b]	Down-regulated genes[b]	Significant shared GO terms[a] for up regulated genes[c]	Significant shared GO terms[a] for down regulated genes[c]
Tyrosol treated vs. Untreated	261	181	Cell surface (16), Cell wall (18), Hyphal cell wall (13), Extracellular matrix (14), Peroxisomal matrix (5), Biofilm matrix (14) Carbohydrate metabolic process (32), Glycolytic process (11), Glycolytic fermentation (4), Purine nucleotide biosynthetic process (12) Response to oxidative stress (18), Oxidoreductase activity (38), Peroxidase activity (5), Cofactor binding (29), Drug catabolic process (8), Positive regulation of defense response (6)	Transmembrane transport (42), rRNA transport (6), Amino acid transport (11), Anion transmembrane transporter activity (14) Cell wall (14), Hyphal cell wall (8), Cytosol (28), Cytosolic ribosome (26) Translation (34), Cytoplasmic translation (12), Ribosome biogenesis (25), Large ribosomal subunit (14), Small ribosomal subunit (12)

[a] - Significant shared GO terms ($p<0.05$) were determined with Candida Genome Database Gene Ontology Term Finder (http://www.candidagenome.org/cgi-bin/GO/goTermFinder). Table contains selected significant shared terms only. The whole data set is available in Supplementary Table 3.

[b] - Up- and down-regulated genes were defined as differentially expressed genes (corrected p value < 0.05) where $\log_2(FC) > 0.585$ or $\log_2(FC) < -0.585$, respectively, and FC stands for fold change FPKM value.

[c] – Figures represent the number of up-regulated or down-regulated genes belonging to the appropriate GO term.

Legends to the Figures

Figure 1

Effect of tyrosol on the growth of *C. parapsilosis*.

Growth of *C. parapsilosis* CLIB 214 was followed in YPD medium by measuring of absorbance (OD_{640}). Tyrosol was added at four hours incubation time at a 15 mM final concentration. Figures represent mean ± SD values calculated from ten independent experiments. Asterix symbols represents significant difference between control and tyrosol-treated cultures calculated by paired Student's *t*-test.

Figure 2

Results of *in vivo* experiments.

Kidney tissue burden of the permanent neutropenic BALB/c mice infected intravenously with the *C. parapsilosis* strain CLIB 214. Daily intraperitoneal tyrosol (15 mM) treatment was started at 24 hours post-inoculation. Fungal kidney tissue burden was determined at the end of the experiments on day six. Bars represent mean ± SD. The level of statistical significance compared with the untreated control group on day six is indicated: $^{**}p < 0.01$.

Figure 3

Correlation between RT-qPCR and transcriptome data.

RNA-Seq data are presented as $\log_2$FC values, where by FC is short for "fold change". Relative transcription levels were quantified with $\Delta\Delta CP = \Delta CP_{control} - \Delta CP_{treated}$. $\Delta CP_{treated} = CP_{\text{test gene}} - CP_{\text{reference gene}}$ measured from treated cultures. $\Delta CP_{control} = CP_{\text{test gene}} - CP_{\text{reference gene}}$ measured from control cultures. CP values represented the qRT-PCR cycle numbers of crossing points. The *ACT1* gene was used as a reference gene. Significantly (Student's *t*-test,

$p < 0.05$, $n = 3$) higher or lower than zero $\Delta\Delta CP$ values (up- or down-regulated genes) are marked with red and blue colours, respectively. The Pearson's correlation coefficient between the RT-qPCR and RNA-seq values was 0.88.

Figure 4

Genome-wide transcriptional changes induced by tyrosol in *C. parapsilosis*

Up-regulated (red) and down-regulated (dark blue) genes were defined as differentially expressed genes (corrected p-value < 0.05) where $\log_2(FC)>0.585$ or $\log_2(FC)< -0.585$, respectively, and FC stands for fold change FPKM value (tyrosol treated *vs*. untreated). Figures, on the sides of the volcano plot, presents representative genes up-regulated or down-regulated by tyrosol treatment.

Supplementary Figure 1: Cluster (A) and principal component (B) analysis of the transcriptome data.

Symbols represent untreated control (Cont) and 15 mM tyrosol exposure (Tyr) cultures. Analyses were performed with the StrandNGS software using default settings.

Supplementary Table 1: Oligonucleotide primers used for RT-qPCR analysis.

Supplementary Table 2: Results of the RT-qPCR measurements.

Relative transcription levels were quantified with $\Delta\Delta CP = \Delta CP_{control} - \Delta CP_{treated,}$ where $\Delta CP_{treated} = CP_{tested\ gene} - CP_{reference\ gene}$ measured from treated cultures and $\Delta CP_{control} = CP_{tested\ gene} - CP_{reference\ gene}$ measured from control cultures. CP values stand for the qRT-PCR cycle numbers of crossing points. RT-qPCR data are presented as mean ± SD calculated from three independent measurements, normalised to the *ACT1* (CPAR2_201570**)** gene expression and

were compared using Student's *t*-test ($p<0.05$). Significantly higher or lower than zero ΔΔCP values (up- or down-regulated gene) are marked with red and blue colours.

Supplementary Table 3: Results of the gene set enrichment analysis.

Significant shared GO terms ($p < 0.05$) were determined with the Candida Genome Database Gene Ontology Term Finder (http://www.candidagenome.org/cgi-bin/GO/goTermFinder). Up- and down-regulated genes were defined as differentially expressed genes where $\log_2(FC) > 0.585$ or $\log_2(FC) < -0.585$ and FC stands for fold change FPKM value. Biological processes, molecular function and cellular component categories are provided. Terms highlighted with yellow are presented in Table 2.

Supplementary Table 4: Transcription data of selected gene groups.

Part 1: Selected genes involved in genetic control of *Candida parapsilosis* virulence.

Part 2: Selected genes involved in glucose catabolism.

Part 3: Selected signal transduction, transmembrane transport, and ribosome biogenesis genes.

Part 4: Selected genes involved in oxidative stress defence.

The systematic names, gene names, gene orthologs in *Candida albicans* and the features (putative molecular function or biological process) of the genes are given according to the Candida Genome Database (http://www.candidagenome.org). Up- and down-regulated genes were defined as differentially expressed genes (corrected p-value < 0.05) where $\log_2(FC)>0.585$ or $\log_2(FC)< -0.585$, respectively, and FC stands for fold change FPKM value (tyrosol treated *vs*. untreated).

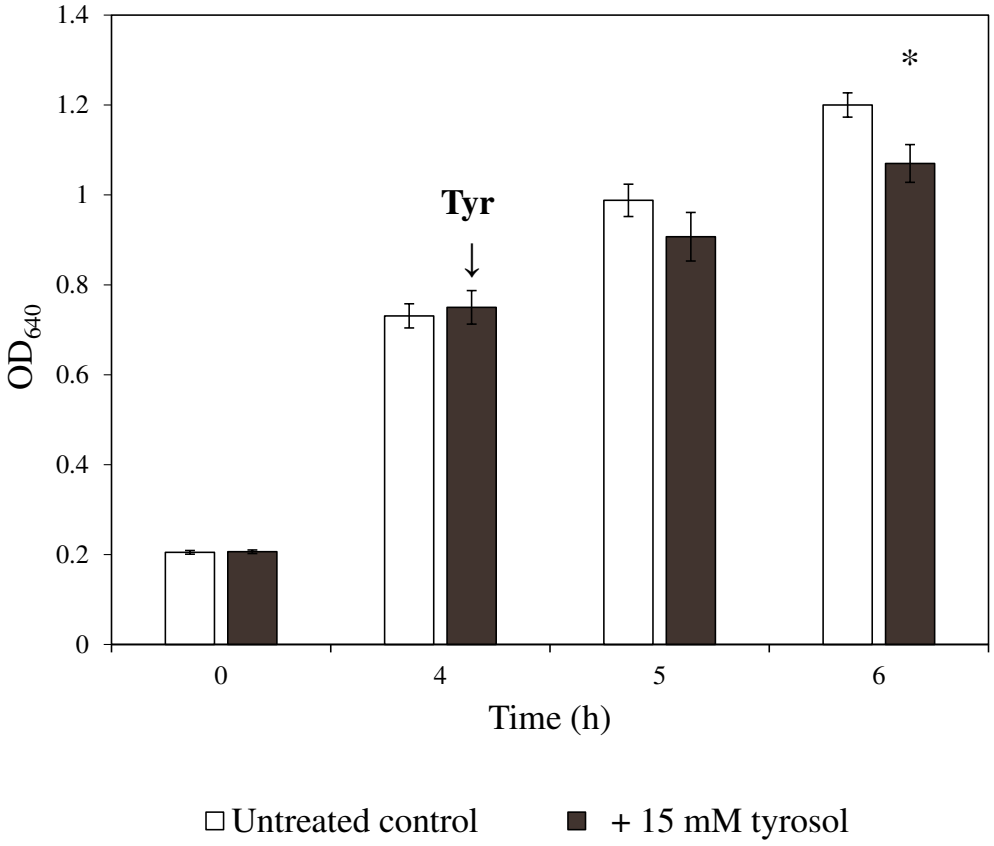
1.4
1.2
1
0.8
0.6
0.4
0.2
0
OD640
Tyr
*
0
4
5
6
Time (h)
Untreated control
+ 15 mM tyrosol

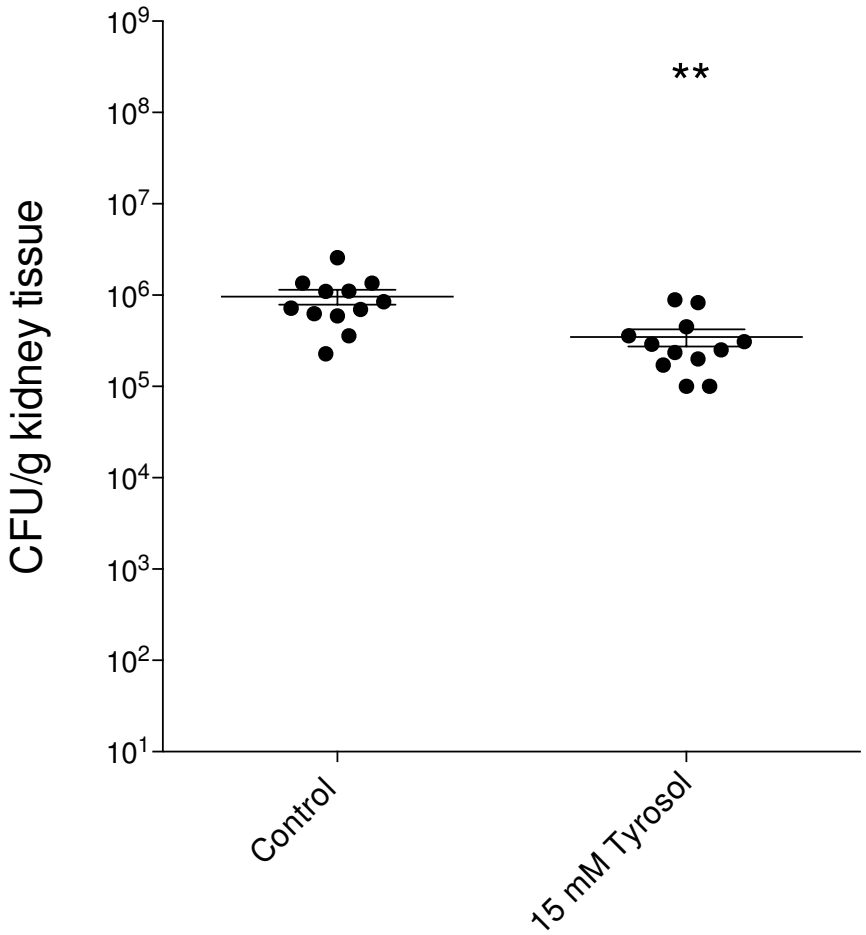
CFU/g kidney tissue
10^9
10^8
10^7
10^6
10^5
10^4
10^3
10^2
10^1
**
Control
15 mM Tyrosol

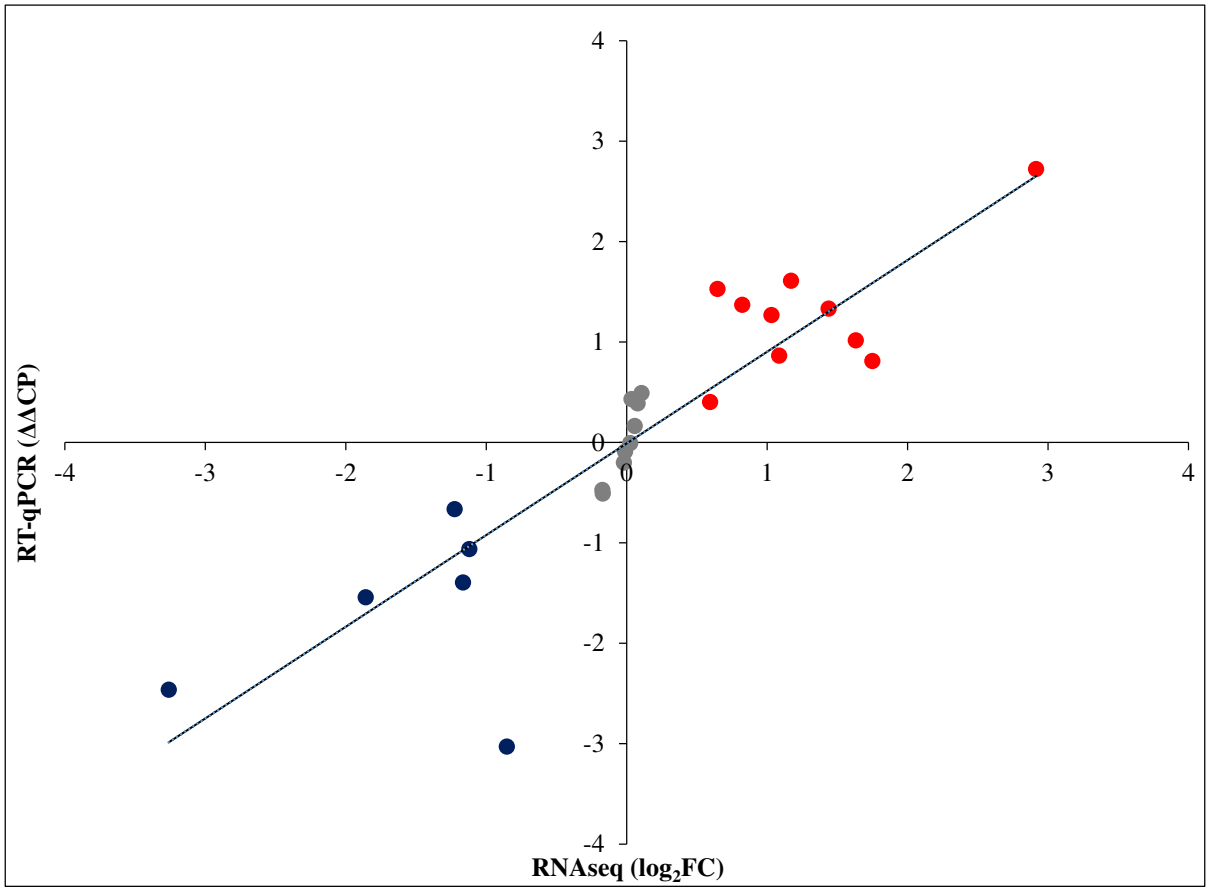
RT-qPCR (ΔΔCP)
RNAseq (log2FC)
4
3
2
1
0
-1
-2
-3
-4
-4
-3
-2
-1
0
1
2
3
4

Adhesion: ALS6
Phospholipase: PLB3
Biofilm: MKC1
Fatty acid metabolism: FAD2, FAD3

Cell wall organization: RHD3, PGA30, IFF6

Ribosome biogenesis
Small subunit genes: RPS3, RPS15, TIF5, YST1 etc.
Large subunit genes: RPL5, RPL8B, RPL25, RPP2A etc.

Transport
Amino acid: GAP1, GAP4, PUT4, DIP5, GNP3, MUP1, AGP3, ARG11, UGA1
Carbohydrate: HGT1, HGT10, HGT13, HGT14, HGT17, YOR1, NGT1, NAG3-4, HXT5
Lactate: JEN2, **Sulfate**:SUL2
Zinc: ZRT2, **Iron**: SIT1
Alcohol: HOL1
Nucleosid: NUP, FCY21

Signal transduction: MKC1, RGS2, PDE2

DOWN (181)

UP (261)

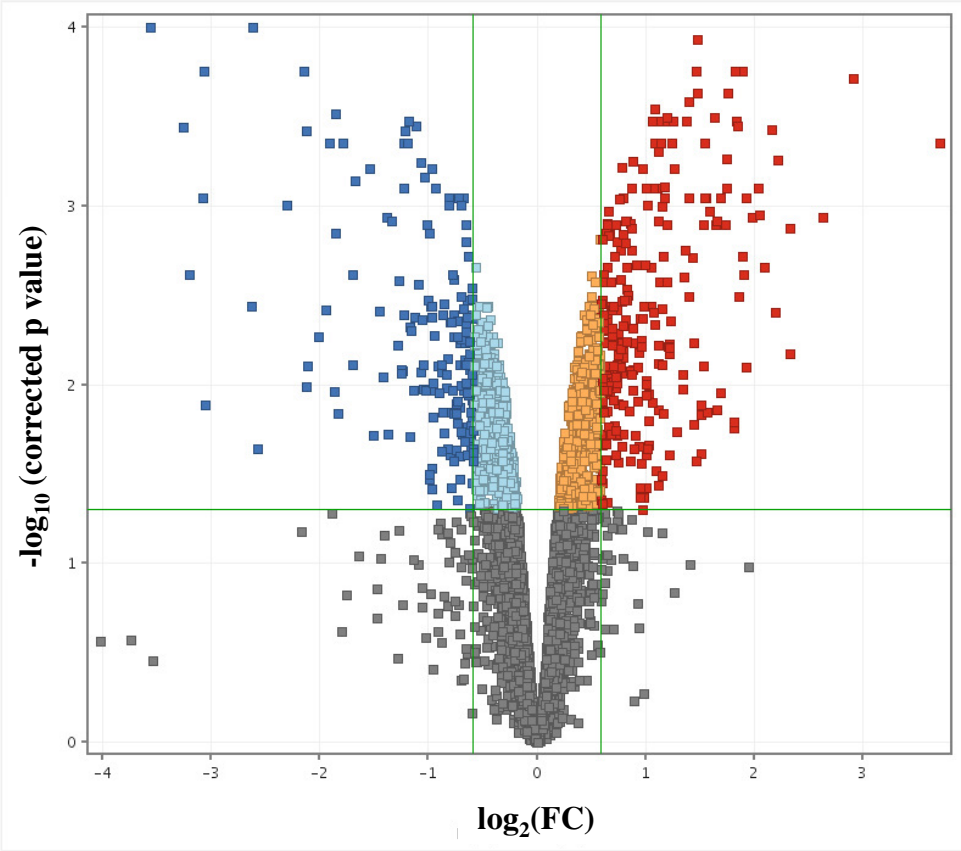

Morphology: CZF1
Biofilm- Maturation: CZF1, RBT1, IFD6, ADH5, TEC1, HGC1
Biofilm- Dispersion: NRG1
Drug transporters: CDR1, MDR1, C1_00830W, CPAR2_405280, FCR1

Cell wall organization: GPH1, EXG2, WSC1, XYL2, GPM2

Glycolysis: PGI1, PFK1, PFK2, TDH3, PGK1, GPM2, ENO1, CDC19
Fermentation: PDC11, PDC12, ADH1, ADH5, ADH7
Glycerol biosyntesis: RHR2

Glutamate metabolism: GDH3

Oxidative stress
Antioxidant enzymes: CAT1, SOD4, CPAR2_803850, GST2, AHP1, GPX1
Regulation and other functions: CAP1, PST1, CIP1, GND1, MSN4, TAC1, SRR1, XBP1, POS5, C3_06860C_A

Signal transduction: RIM101, MSB2, DPL1, SRR1, CPP1, PHO84